Intercellular Ca^{2+} Wave Propagation through Gap-Junctional Ca^{2+} Diffusion: A Theoretical Study

Thomas Höfer, Antonio Politi, and Reinhart Heinrich
Theoretical Biophysics, Institute of Biology, Humboldt University-Berlin, D-10115 Berlin, Germany

ABSTRACT Intercellular regenerative calcium waves in systems such as the liver and the blowfly salivary gland have been hypothesized to spread through calcium-induced calcium release (CICR) and gap-junctional calcium diffusion. A simple mathematical model of this mechanism is developed. It includes CICR and calcium removal from the cytoplasm, cytoplasmic and gap-junctional calcium diffusion, and calcium buffering. For a piecewise linear approximation of the calcium kinetics, expressions in terms of the cellular parameters are derived for 1) the condition for the propagation of intercellular waves, and 2) the characteristic time of the delay of a wave encountered at the gap junctions. Intercellular propagation relies on the local excitation of CICR in the perijunctional space by gap-junctional calcium influx. This mechanism is compatible with low effective calcium diffusivity, and necessitates that CICR can be excited in every cell along the path of a wave. The gap-junctional calcium permeability required for intercellular waves in the model falls in the range of reported gap-junctional permeability values. The concentration of diffusive cytoplasmic calcium buffers and the maximal rate of CICR, in the case of inositol 1,4,5-trisphosphate (IP_3) receptor calcium release channels set by the IP_3 concentration, are shown to be further determinants of wave behavior.

INTRODUCTION

The elevation of the cytoplasmic calcium concentration is a central step in many intracellular signal transduction pathways (e.g., Thomas et al., 1996; Berridge, 1997). Recently, it has been observed in various systems that calcium signals can also mediate intercellular communication by eliciting or coordinating calcium signals in surrounding cells, for example in the liver (Robb-Gaspers and Thomas, 1995; Patel et al., 1999), and the astrocyte networks of the central nervous system (Cornell-Bell et al., 1990; Giaume and Venance, 1998). Two general pathways of intercellular calcium signaling have been identified: the diffusion of cytoplasmic messenger molecules through gap junctions (e.g., Charles et al., 1992; Giaume and McCarthy, 1996; Tjordmann et al., 1997; Toyofuku et al., 1998; Domenighetti et al., 1998), and the secretion of extracellular messengers (Hassinger et al., 1996; Schlosser et al., 1996).

Both the calcium-releasing messenger inositol 1,4,5-trisphosphate (IP_3) and calcium can participate in the gap-junctional mode of transmission (Sáez et al., 1989; Christ et al., 1992). In some systems, such as the airway epithelium, a stimulus applied to a single cell elevates IP_3 through activation of phospholipase C (PLC). IP_3 is thought to diffuse from the stimulated cell and trigger calcium release in surrounding cells. (Sanderson, 1995; Sneyd et al., 1995). In other systems, an external signal linked to PLC activation is applied globally, so that IP_3 concentration increases in practically all cells. Under these conditions, calcium has been hypothesized to act as an intercellular mediator, e.g., in pancreatic acini (Yule et al., 1996), chondrocytes (D'Andrea and Vittur, 1997), hepatocytes (Robb-Gaspers and Thomas, 1995), and the blowfly salivary gland (Zimmermann and Walz, 1999). This appears feasible, as calcium liberation from the endoplasmic reticulum (ER) can be activated by calcium in the presence of IP_3 receptor calcium release channels (IP_3R) that are sensitized by IP_3 (Bezprozvanny and Ehrlich, 1995), and potentially also ryanodine receptor channels (RyR; Meissner, 1994). We refer to this phenomenon for both sensitized IP_3R and RyR as calcium-induced calcium release (CICR). In the presence of CICR, calcium influx through gap junctions may trigger calcium release in a cell and in this way a regenerative intercellular calcium wave could spread. Given the occurrence of CICR and gap junctions in many systems, this may be a basic mechanism of intercellular calcium signaling. However, up to now little is known about the requirements on the various cellular calcium transport processes that would enable gap-junctional calcium fluxes to propagate a calcium signal.

The understanding of the interaction of these processes can be greatly facilitated by mathematical modeling. Recently, models based on a CICR/gap-junctional calcium diffusion mechanism were developed for the formation of intercellular spiral waves of calcium in hippocampal slices (Wilkins and Sneyd, 1998), and for the synchronization of calcium oscillations in hepatocyte couplets (Höfer, 1999). A common finding of these mainly numerical studies is the existence of a critical junctional calcium permeability, which must be exceeded for intercellular wave propagation or synchronization. The calcium kinetics in the two models assume two different mechanisms of the decline of calcium concentration, both of which have been implicated in experimental studies: slow inactivation of the IP_3R (Wilkins and Sneyd, 1998) and decrease of the total calcium content

Received for publication 16 May 2000 and in final form 23 October 2000.
Address reprint requests to Dr. Thomas Höfer, Dept. of Theoretical Biophysics, Institute of Biology, Humboldt University-Berlin, Invalidenstrasse 42, D-10115 Berlin, Germany. Tel.: 49-30-2093-8592; Fax: 49-30-2093-8813; E-mail: thomas.hoefer@rz.hu-berlin.de.

0006-3495/01/01/75/13 $2.00

of the cell (Höfer, 1999). However, it appears that the calcium wavefronts primarily propagate through the interaction of CICR and calcium diffusion, so that the waves should have common properties irrespective of the particular dynamics in their wakes. In the present paper we thus study a model of calcium elevation through CICR coupled to cytoplasmic and gap-junctional calcium diffusion.

The model considers a linear cell array and accounts for the following calcium transport and binding processes: 1) CICR from the calcium stores of the ER; 2) removal from the cytoplasm; 3) buffering by calcium binding to proteins, lipids, and other molecules; 4) cytoplasmic diffusion; and 5) in the perijunctional space, calcium fluxes across the gap junctions. Many of the parameters of these processes can vary, and their variation may affect intercellular wave propagation. In the presence of IP_3R, the maximal rate of CICR is a function of the IP_3 concentration that depends on the amount of PLC-activating external agonist. The composition of calcium buffers in the cell can be regulated and also altered experimentally (e.g., Wang et al., 1997). Moreover, all parameters may vary with cell type and conditions, particularly pertinent to the study of intercellular signals being the regulation of gap-junctional permeability (Bruzzone et al., 1996).

The analysis of the model will focus on the conditions under which intercellular calcium waves can occur, and on how the occurrence and properties of the waves depend on the parameters of the calcium transport processes in the cell. We are aware that a detailed representation of these processes requires considerably more complex models. However, the present paper is aimed at elucidating characteristics of the CICR/calcium diffusion mechanism in terms of basic cellular parameters. The results may inform experimental studies and more detailed modeling approaches to specific systems.

MODEL

Model equations and parameters

Consider the linear array of cells depicted in Fig. 1. The concentration of cytoplasmic calcium, in the ith cell, $[Ca^{2+}_{cyt,i}] = u_i(x, t)$, $i = 0, 1, \ldots, n$, is governed by the rates of calcium release from the ER and removal from the cytoplasm, $f(u_i)$, and by cytoplasmic diffusion with an effective diffusion coefficient D,

$$\frac{\partial u_i}{\partial t} = h(x)f(u_i) + D\frac{\partial^2 u_i}{\partial x^2}, \quad 0 \le x \le L. \tag{1}$$

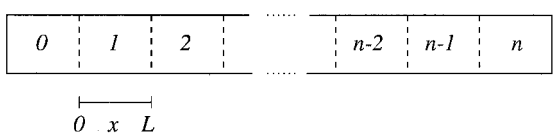

FIGURE 1 Linear array of cells of uniform length, L, coupled by gap junctions.

where L denotes the length of a cell and x is mapped for each cell individually to the interval $(0, L)$. The function $h(x)$ refers to the spatial distribution of calcium release/uptake sites.

During an intercellular calcium signal, calcium remains elevated for some time, usually some tens of seconds, as the signal spreads to neighboring cells, usually within seconds. We study the advance of the front of the signal and, for simplicity, assume that a (quasi-) stationary state of high calcium concentration is attained in the wake of the front. This can be described by the rate expression

$$f(u) = v_m\frac{u^\nu}{K_a^\nu + u^\nu} - ku, \tag{2}$$

with v_m and K_a denoting the maximal rate and half-saturation constant of CICR, respectively, and k being a "lumped" rate constant of calcium removal from the cytoplasm. Hill coefficients between 1.2 and 3.5 have been used to fit data for IP_3R (Bezprozvanny and Ehrlich, 1995; Dufour et al., 1997); subsequently we take $\nu = 2$. To carry out mathematical analysis of the model, we also consider a piecewise linear (p.w.l.) approximation to Eq. 2, corresponding to the limit $\nu \to \infty$,

$$f(u) = v_m H(u - K_a) - ku, \tag{3}$$

where $H(\cdot)$ is the Heaviside step function. Equations 2 and 3 have previously been used as simple rate expressions for CICR (e.g., Murray, 1993). The width of a cytoplasmic calcium wavefront is about one to several micrometers. On this scale, we assume a homogeneous distribution of calcium release and uptake sites, $h(x) = 1$. However, before a calcium wave is initiated, a distance d between the gap junctions and the ER may have to be bridged solely by diffusion. To reflect this in a simple manner, we take

$$h(x; d) = \begin{cases} 0; & 0 < x < d \quad \text{and} \quad L - d < x < L \\ 1; & d \le x \le L - d, \end{cases} \tag{4}$$

where d is the distance between gap junctions and calcium stores, $0 \le d < L/2$.

The intercellular calcium fluxes are assumed proportional to the concentration differences across the gap junctions,

$$-D\frac{\partial u_i}{\partial x}\bigg|_{x=0} = P[u_{i-1}(L, t) - u_i(0, t)],$$

$$D\frac{\partial u_i}{\partial x}\bigg|_{x=L} = P[u_{i+1}(0, t) - u_i(L, t)], \tag{5}$$

where P is the effective gap-junctional calcium permeability.

Cytoplasmic calcium is bound to many molecules, leading to a substantial buffering of its concentration. Equations 1 and 5 include the effect of buffering via a rapid-equilibrium approximation, assuming that calcium binding is fast compared to the rates of CICR, calcium removal, and buffer molecule diffusion, and that the buffers are not saturated by calcium binding. These are reasonable assumptions for a large class of buffering molecules (Neher and Augustine, 1992; Wagner and Keizer, 1994). In Appendix 1 it is shown that the calcium dynamics are then governed by Eqs. 1 and 5 with an effective rate of calcium release/removal $f(u)$, an effective diffusion coefficient D, and an effective junctional calcium permeability P, defined as

$$f(u) = \frac{f_0(u)}{1 + \sum_{j=1}^{M} B_j/K_j},$$

$$D = \frac{D_0 + \sum_{j=1}^{M} D_j B_j/K_j}{1 + \sum_{j=1}^{M} B_j/K_j},$$

$$P = \frac{P_0}{1 + \sum_{j=1}^{M} B_j/K_j}, \tag{6}$$

where B_j, K_j, and D_j denote the total concentration of the calcium binding sites of the buffer species j, their dissociation constant, and the diffusion coefficient of the buffer species j, respectively. D_0, $f_0(u)$, and P_0 are the respective values the diffusion coefficient of calcium, its release/removal rate, and its junctional permeability would attain in the absence of buffers. Values of $\Sigma_j B_j/K_j$ range between 20 and 100 in various cell types (Neher and Augustine, 1992; Daub and Ganitkevitch, 2000).

Typical ranges for the parameters are given in Table 1; the values may vary with the particular system. In the case of IP_3R, v_m increases with the IP_3 concentration. D specifically depends on the concentration of diffusive calcium buffers, for which $D_j > 0$. This reflects that calcium may diffuse bound to buffers and then be released. P_0 depends on the number, distribution, type, and state of the gap junctions, and on the permeating molecule. The quoted values of P_0, obtained for molecules other than calcium and in specific cell types, are taken to indicate the accessible range. $\Sigma_j B_j/K_j$ of 20–100 yields P between 0.01 and 0.15 μm/s (Eq. 6).

Limitations of the model

The rate functions Eqs. 2 and 3 are substantially simplified compared to other models of cellular calcium dynamics. Of relatively little consequence is the neglect of a small leak flux of calcium into the cytoplasm, causing the resting calcium level in the model to be zero, rather than at a concentration of 50–100 nM. Inclusion of a leak would not affect the results, so that we have not done so. It is also assumed that the calcium concentration in the ER is negligibly reduced by calcium release, rendering the release rate a function of only cytoplasmic calcium. Moreover, the inactivation of the IP_3R by very high calcium concentrations is not included. As a consequence of the latter two assumptions, the model can describe the leading front, but not the falling phase, of a calcium signal. Such a description is reasonable if the time scales of intercellular spread and slower decline of the signal separate. The model is found to overestimate the peak calcium concentrations for values of v_m and k that give realistic intracellular calcium wave speeds, reaching 1–3 μM, rather than the measured values of 500 nM − 1 μM, probably owing to the neglect of inactivating processes. The various calcium removal processes from the cytoplasm (primarily uptake into ER and mitochondria, near the plasma membrane also efflux from the cell) have been lumped into a single linear removal rate, ku. In real systems, saturation effects at higher calcium concentration will play a role; however, at least for small concentration changes, such as through gap-junctional calcium influx, saturating rate laws can be linearized. An assumption implicit in the spatially one-dimensional formulation of the calcium diffusion fluxes in Eqs. 1 and 5 is an overall homogeneous distribution of gap junction channels across the plasma membranes at cell contacts.

TABLE 1 Parameter values

Parameter	Value	Reference
D	10–40 $\mu m^2/s$	Allbritton et al. (1992)
P_0	1–3 μm/s	Verselis et al. (1986), Eckert et al. (1999)
v_m, k	1–20 μM/s, 1/s	Mathematical models, e.g., Dupont and Goldbeter (1993), Sneyd et al. (1995)
K_a	200 nM	Kaftan et al. (1997), Hagar et al. (1998), (IP_3R); Fabiato (1985) (RyR)

ANALYSIS

The analysis is simplified by obtaining suitable parameter groupings from the model parameters. We introduce the scaled time $\tau = kt$, space $\xi = x/L$, and calcium concentration $\tilde{u} = u/K_a$. For continuity, we will use the symbol $u(\xi, \tau)$ instead of $\tilde{u}$ for the scaled concentration; it will be set apart from the unscaled concentration by the independent variables. The model takes the form

$$\frac{\partial u_i}{\partial \tau} = h(\xi; l)g(u) + \delta \frac{\partial^2 u_i}{\partial \xi^2}, \quad 0 \le \xi \le 1, \tag{7}$$

$$-\delta \frac{\partial u_i}{\partial \xi}\bigg|_{\xi=0} = p[u_{i-1}(1, \tau) - u_i(0, \tau)],$$
$$\delta \frac{\partial u_i}{\partial \xi}\bigg|_{\xi=1} = p[u_{i+1}(0, \tau) - u_i(1, \tau)], \tag{8}$$

$$g(u) = \alpha \frac{u^2}{1 + u^2} - u, \tag{9a}$$

$$g(u) = \alpha H(u - 1) - u, \tag{9b}$$

with the smooth and p.w.l. kinetics, respectively; $h(\xi; l)$ is given by Eq. 4 with $l = d/L$. The three dimensionless parameter groupings are

$$\alpha = v_m/(kK_a), \quad \delta = D/(kL^2), \quad p = P/(kL). \tag{10}$$

With Eq. 6 we obtain

$$\alpha = \frac{v_{m,0}}{k_0 K_a}, \quad \delta = \frac{D_0 + \sum_{j=1}^{M} D_j B_j/K_j}{k_0 L^2},$$
$$p = \frac{P_0}{k_0 L}, \tag{11}$$

where $v_{m,0}$ and k_0 are the values of the rate constants in the absence of buffering. The behavior of the scaled model is independent of the concentrations of non-diffusive calcium buffers (for which $D_j = 0$).

Equations 7 and 8 can be approximated by a simpler set of equations for the average cytoplasmic calcium concentrations, $U_i(\tau) = \int_0^1 u_i(\xi, \tau)d\xi$, if the diffusion rate over the length of the cell is much greater than the rates of calcium release and of the junctional fluxes. In the corresponding limit $\alpha/\delta \to 0$ and $p/\delta \to 0$, Eqs. 7 and 8 can be shown to be equivalent to

$$\frac{dU_i}{d\tau} = (1 - 2l)g(U_i) + p(U_{i-1} - 2U_i + U_{i+1}). \tag{12}$$

From Table 1 and assuming a cell length of 10 μm, the following ranges for α, δ, and p are obtained: $5 < \alpha < 50$, $0.1 < \delta < 0.4$, and $0.001 < p < 0.015$. Therefore, the compartmental approximation Eq. 12 is not reasonable for our model. It is useful as a point of reference in the analysis.

The kinetics of CICR and calcium removal exhibit bistability, provided $\alpha > 2$ for Eq. 9a and $\alpha > 1$ for Eq. 9b (Fig. 2). The upstroke of a calcium signal is represented by the transition from the rest state $u = 0$ to the excited state u_a; a moving transition front corresponds to the front of a calcium wave.

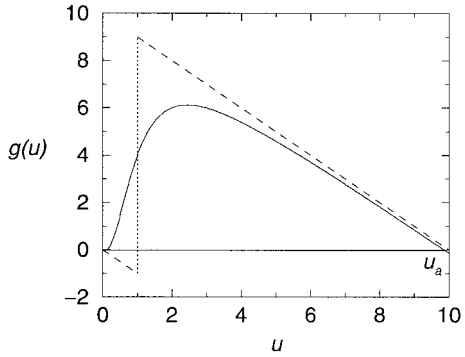

FIGURE 2 Bistable kinetics of ER calcium release and removal $g(u)$, with sigmoid CICR function (Eq. 9a), solid line, and step-function CICR (Eq. 9b), dashed line; $\alpha = 10$. The states $u = 0$ and $u = u_a$ correspond to the rest state of low cytoplasmic calcium and the elevated calcium level following the triggering of CICR, respectively. Quantitatively comparable results for both types of rate functions are obtained below if the threshold for CICR in the p.w.l. kinetics is adjusted to be equal to the unstable steady state of the smooth rate function by assuming a smaller K_a for Eq. 9b, and correspondingly a larger value of α.

Suppose that initially the calcium concentration in all cells is at the rest state, $u_i(x, 0) = 0$, and that a local stimulus is applied in cell 0, at $x = 0$,

$$u_0(0, \tau) = s, \quad \tau > 0. \tag{13}$$

The calcium level is thought to remain elevated sufficiently long to assume s constant. Local initiation has been observed in liver lobules at sites of particularly high hormone sensitivity (Tordjmann et al., 1998), and in the blowfly salivary gland after calcium injection (Zimmermann and Walz, 1999). If the stimulus triggers a regenerative intercellular calcium wave, eventually all cells of the array become activated. However, it may be possible that signal propagation fails at some distance from the point of initiation, because the gap-junctional calcium influx into a cell becomes too small to excite CICR. In such a case the spatial range of the signal remains limited. The asymptotic behavior, $\tau \to \infty$, in the limit of a semi-infinite cell array, $0 \le i < \infty$, yields

$$\lim_{i\to\infty} u_i(\xi) = u_a, \tag{14a}$$

$$\lim_{i\to\infty} u_i(\xi) = 0, \tag{14b}$$

for regenerative intercellular calcium waves and spatially limited calcium signals, respectively. Here the $u_i(\xi)$ denote stationary concentrations. If a stationary profile satisfying the boundary conditions 13 and 14b exists, we have observed that the $u_i(\xi, \tau)$ approach this solution after application of a local stimulus s. Therefore, regenerative intercellular calcium waves are not found in this case. The solutions to Eq. 12 with bistable kinetics have an analogous property; it can be used to obtain a condition for regenerative wave propagation (Keener, 1987).

The calculations can be done explicitly with the p.w.l. kinetics Eq. 9b. To guarantee initiation of a calcium signal within a cell, we assume $s > 1$, and spreading intracellular calcium waves to exist, yielding, from the condition $\int_0^{u_a} g(u)\, du > 0$ (cf. Murray, 1993), $\alpha > 2$. Stationary solutions to Eqs. 7 and 8 with 9b may satisfy Eqs. 13 and 14b, if calcium in cells up to cell m, $m \ge 0$, is above the CICR threshold, while in the remaining cells it is below:

$$u_i(\xi)\begin{cases} > 1 & 0 \le i \le m \\ < 1 & m+1 \le i < \infty. \end{cases} \tag{15}$$

Letting $\partial u_i/\partial\tau = 0$ in Eq. 7 yields the following ansatz for the calcium profiles,

$$u_i(\xi) = \begin{cases} \alpha_i + \beta_i + \gamma_i + \dfrac{1}{\sqrt{\delta}}(-\beta_i + \gamma_i)(\xi - l); & 0 < \xi < l \\ \alpha_i + \beta_i e^{-(\xi-l)/\sqrt{\delta}} + \gamma_i e^{(\xi-l)/\sqrt{\delta}}; & l \le \xi \le 1 - l \\ \alpha_i + \beta_i\rho + \gamma_i/\rho + \dfrac{1}{\sqrt{\delta}}(-\beta_i\rho + \gamma_i/\rho)\xi; & 1 - l < \xi < 1, \end{cases} \tag{16}$$

where $\alpha_i = \alpha$ if $0 \le i \le m$ and zero otherwise, $\rho = e^{-(1-2l)/\sqrt{\delta}}$, and continuity of u_i and $\partial u_i/\partial\xi$ at $\xi = l$ and $\xi = 1 - l$ is ensured. Joining the solutions for neighboring cells through Eqs. 8, one obtains a linear system of difference equations for β_i and γ_i, of the form $(\beta_{i+1}, \gamma_{i+1})^T = A(\beta_i, \gamma_i)^T$; the matrix A results from evaluating Eqs. 8 with Eq. 16 for $i < m$ and $i > m + 1$. It is solved by

$$\beta_i = b_1\lambda^i + b_2\lambda^{-i}, \quad \gamma_i = \nu_1 b_1\lambda^i + \nu_2 b_2\lambda^{-i}; \qquad 0 \le i \le m \tag{17}$$

$$\beta_i = B_1\lambda^i, \quad \gamma_i = \nu_1 B_1\lambda^i; \quad m+1 \le i < \infty, \tag{18}$$

with

$$\lambda = T(1 - \sqrt{1 - 1/T^2}),$$
$$T = \cosh\left(\frac{1-2l}{\sqrt{\delta}}\right) + \left(\frac{l}{\sqrt{\delta}} + \frac{\sqrt{\delta}}{2p}\right)\sinh\left(\frac{1-2l}{\sqrt{\delta}}\right), \tag{19}$$

$\nu_1 = (\rho - \lambda)/(1/\rho - \lambda)$, and $\nu_2 = (\rho\lambda - 1)/(\lambda/\rho - 1)$. It is straightforward to show that λ is real and $0 \le \lambda \le 1$. In Eq. 18 we have applied the boundary condition Eq. 14b, excluding λ^{-i}-terms.

Using Eqs. 17 and 18 with Eq. 16 to evaluate the gap-junctional flux conditions Eq. 8 between cells m and $m + 1$, and the left boundary condition Eq. 13, a linear system of equations for b_1, b_2, and B_1, as a function of m, is obtained. This generally has a unique solution. In this way, the coefficients β_i and γ_i in Eq. 16 are found in terms of the model parameters, with the spatial range of the signal m to be determined. Consistency of the solution with relation 15 yields m such that

$$u_m(l) > 1, \quad u_{m+1}(l) < 1 \tag{20}$$

are fulfilled.

A critical situation occurs if the calcium concentration in cell $m + 1$ just reaches the CICR threshold at the location of the calcium stores: $u_{m+1}(l) = 1$. This condition separates the case of the $(m + 1)$st cell being not excited from the case of it becoming excited. For $u_{m+1}(l)$ one obtains

$$u_{m+1}(l) = \frac{2}{\mathcal{D}} p\lambda(1 + \nu_1)(1 - \rho\lambda) \times \{2\lambda^m\rho(\nu_1 - \nu_2)(\alpha - s) + \alpha[(l_1 + \nu_1 l_2)(\nu_2 - \rho^2) - \lambda^{2m}(l_1 + \nu_2 l_2)(\nu_1 - \rho^2)]\}, \tag{21}$$

where $l_{1,2} = 1 \pm l/\sqrt{\delta}$ and

$$\begin{aligned}\mathcal{D} = l_1(1+\nu_1)\{&-\sqrt{\delta}\lambda(\nu_2-\rho^2)(\rho^2-1)\\ &+2p[\rho(\nu_2-\rho^2)-\lambda(\nu_1-1)(l_1\nu_2+\rho^2 l_2)\\ &+\lambda^2\rho((l_1(\nu_1-1)-1)\nu_2+(l_2(\nu_1-1)+1)\rho^2)]\}\\ +\lambda^{2m}l_1(1+\nu_2)\{&\sqrt{\delta}\lambda(\nu_1-\rho^2)(\rho^2-1)\\ &+2p[\rho(\nu_1-\rho^2)+\lambda(\nu_1-1)(l_1\nu_1+\rho^2 l_2)\\ &-\lambda^2\rho((l_1(\nu_1-1)-1)\nu_1+(l_2(\nu_1-1)+1)\rho^2)]\}\end{aligned}$$

If only a limited number of cells becomes excited, then $u_{m+1}(l) < 1$ for some finite value of m. Conversely, if $\lim_{m\to\infty} u_{m+1}(l) > 1$, then the solution satisfies Eq. 14a instead of Eq. 14b, since $u_i \to \alpha$, as $i \to \infty$. In this case, we expect the stimulus to evoke nondecaying intercellular calcium waves. The critical condition separating the two cases is

$$\lim_{m\to\infty} u_{m+1}(l) = 1. \tag{22}$$

Taking the limit $m \to \infty$ in Eq. 21, we observe that the condition for propagation, Eq. 22, depends on the cellular parameters α, p, δ, and l, but not on the size of the initiating stimulus s.

In the special case $l = 0$ (no gap between gap junctions and calcium stores), Eq. 22 yields

$$\frac{\lambda(\cosh(1/\sqrt{\delta})-\lambda)}{1-\lambda^2} = \frac{1}{\alpha}. \tag{23}$$

In the limit $\delta \to \infty$, Eq. 23 can be solved for the critical junctional permeability p_c required for wave propagation. The limiting critical permeability is obtained as

$$p_{c,\infty} = \lim_{\delta\to\infty} p_c = \frac{\alpha-1}{(\alpha-2)^2}, \tag{24}$$

in agreement with direct analysis of the compartmental Eq. 12 (cf. Keener, 1987). Recall that $\alpha > 2$. The parameter estimates suggest the limit of small δ to be appropriate for calcium waves. By expanding the square root in Eq. 19 for large T, we obtain from Eq. 23,

$$p_c \to p_{c,0} = \frac{\sqrt{\delta}}{\alpha-2} \quad \text{as } \delta \to 0. \tag{25}$$

The critical junctional permeability is a monotonically increasing function of δ, initially given by Eq. 25 and approaching $p_{c,\infty}$ (cf. Fig. 3 *a*). Equation

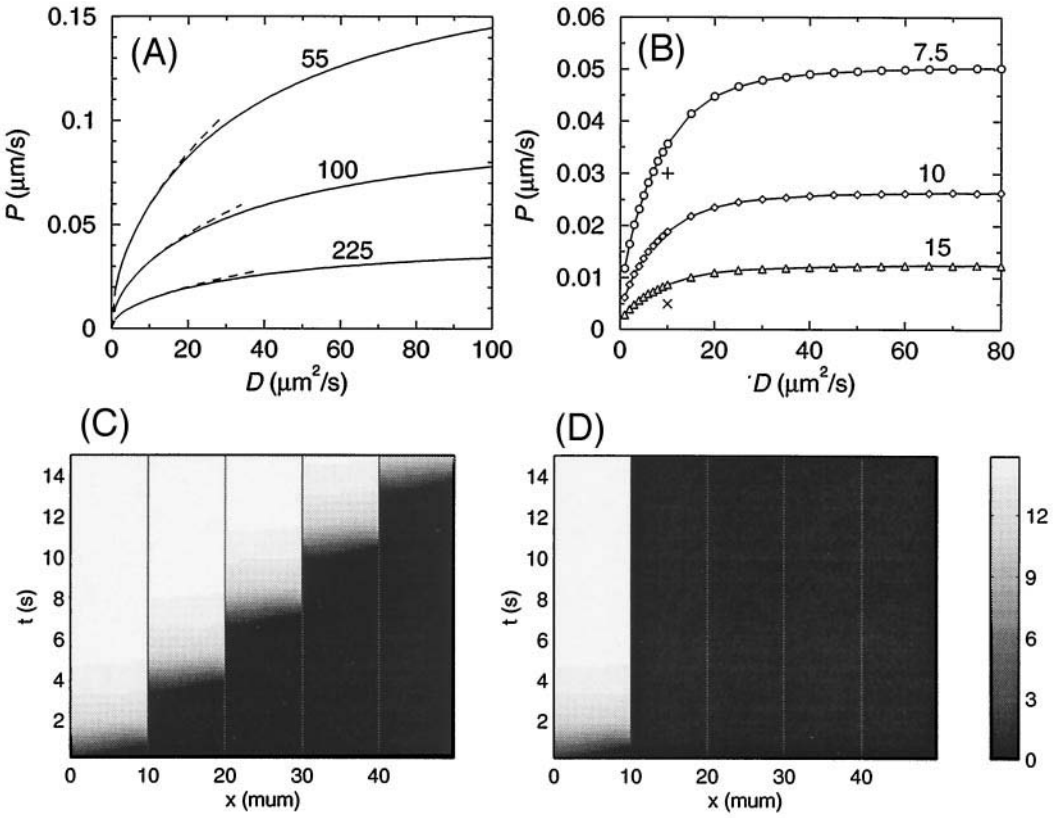

FIGURE 3 Critical gap-junctional permeability P_c required for intercellular calcium wave propagation. (*a*) P_c for p.w.l. kinetics (Eq. 9b) according to Eq. 23 (*solid lines*) and Eq. 25 (*dashed lines*); (*b*) P_c for smooth kinetics (Eq. 9a), calculated numerically at the points indicated. Results for three different values of α as given at the curves; values in (*a*) are chosen to obtain the same CICR thresholds as in (*b*) (cf. Fig. 2). (*c*) Space-time plot of the calcium concentration for intercellular wave (Eq. 9a with $\alpha = 15$, $D = 10$ μm^2/s, $P = 0.03$ μm/s, + in *b*); (*d*) propagation failure ($P = 0.005$ μm/s, × in *b*). The leftmost cell was stimulated and the first 5 of an array of 10 cells are shown. The nondimensional δ and p have been converted to D and P, assuming $L = 10$ μm, $k = 1$/s; calcium concentration scale in dimensionless units.

25 was also obtained in the analysis of a pair of "semi-infinite" cells (Wilkins and Sneyd, 1998).

It is also of interest how fast CICR becomes excited by gap-junctional calcium influx. Assume that in a cell calcium is at its resting concentration, while in a neighboring cell it has attained an elevated level, with concentration $\hat{u}$ immediately at the gap-junctional contact of the two cells. To be specific, let $l = 0$ and the cell to become excited at its left end, $\xi = 0$. The initial calcium rise before the triggering of CICR, $u(\xi, \tau) < 1$, can be approximated by Eq. 7 subject to the initial and boundary conditions

$$u(\xi, 0) = 0, \quad -\delta \left.\frac{\partial u}{\partial \xi}\right|_{\xi=0} = p[\hat{u} - u(0, \tau)], \qquad \lim_{\xi\to\infty} u(\xi, \tau) = 0, \tag{26}$$

with $g(u) = -u$. Following, e.g., Crank (1975), the solution of this problem is obtained, in dimensional quantities, as

$$\frac{u(x, t)}{\hat{u}} = \frac{P}{2}\left[\frac{e^{-x\sqrt{k/D}}}{\sqrt{kD} + P}\,\mathrm{erfc}\left(\frac{x}{2\sqrt{kD}} - \sqrt{kt}\right) - \frac{e^{x\sqrt{k/D}}}{\sqrt{kD} - P}\,\mathrm{erfc}\left(\frac{x}{2\sqrt{kD}} + \sqrt{kt}\right)\right] + \frac{P^2 e^{(P^2/D - k)t + Px/D}}{kD - P^2}\,\mathrm{erfc}\left(\frac{x}{2\sqrt{kD}} - \sqrt{P^2 t/D}\right). \tag{27}$$

The steady state $\bar{u}(x)$ is given by

$$\frac{\bar{u}(x)}{\hat{u}} = \frac{Pe^{-x\sqrt{k/D}}}{\sqrt{kD} + P}, \tag{28}$$

indicating that the right boundary condition in Eqs. 26 is a reasonable approximation if $L(k/D)^{1/2} \gg 1$. We found good agreement between Eq. 27 and numerical solutions on a finite domain with $L(k/D)^{1/2} = 4$.

The approach to the steady state is monotonic at any space point. The characteristic time for the transition to the steady state is in the range of 0.5 s for the parameters of Table 1. It is possible to obtain the parameter dependence of the transition time, t_s. According to the definition of transition time by (Lloréns et al., 1999), we take $t_s(x) = \int_0^\infty (1 - u(x, t)/\bar{u}(x))dt$, yielding $t_s(0) = \sqrt{kD}/[2k(P + \sqrt{kD})]$ at the gap junctions.

RESULTS

Condition for propagation of intercellular waves

Intuitively, intercellular calcium wave propagation requires sufficiently strong gap-junctional coupling of the cells. In the model, an explicit condition for intercellular regenerative wave propagation is established for p.w.l. kinetics (Eq. 9b). We consider first the case of gap junctions and calcium stores being very close ($d = 0$ in Eq. 4). Equation 23 then yields a critical gap-junctional calcium permeability for wave propagation, P_c. P_c is a function of the other parameters; in Fig. 3 *a* its dependence on the effective calcium diffusivity is depicted. For better comparison with experimental data, in this and all following figures the nondimensional values p and δ have been converted to P and D, assuming $L = 10$ μm and $k = 1$/s. For realistic values of the cytoplasmic calcium diffusivity, the propagation condition is approximated by

$$P_{c,0} = \frac{\sqrt{kD}}{v_m/kK_a - 2} \tag{29}$$

(Eq. 25 with dimensional parameters). Corresponding numerical results for the rate equation 9a give the same kind of critical curve (Fig. 3 *b*, Appendix 2). For $P > P_c$, a local stimulus triggers a regenerative intercellular calcium wave (Fig. 3 *c*). It consists of a succession of intracellular waves punctuated by gap-junctional delays, as observed experimentally. If $P < P_c$, no regenerative intercellular waves exist (Fig. 3 *d*). The values for P_c fall in the range of effective calcium permeabilities indicated by experimental data (Table 1).

Interestingly, the critical permeability for intercellular waves decreases with decreasing effective calcium diffusivity D, $P_c \sim \sqrt{D}$ for small D. This dependence indicates that CICR is triggered locally in the perijunctional space. For small values of D, inflowing calcium remains more localized (cf. Eq. 28), and smaller gap-junctional calcium influx is required to reach the CICR threshold near the gap junctions than for large D.

In the example for the failure of intercellular wave propagation given in Fig. 3 *d*, the signal does not propagate beyond the stimulated cell. However, a certain number of neighboring cells might still be excited, if the propagation condition 23 is not satisfied. In the analysis of the p.w.l. model, this is given by the number m ($m \geq 0$), determined by the inequalities 20. To calculate m, values of the calcium concentration s in the stimulated cell are chosen comparable to the calcium amplitude reached upon triggering of CICR, $u_a = \alpha$ in the p.w.l. model. Then parameter regions of seizable extent exist for only two cases of finite m: no cells and 1 cell, the immediate neighbor of the stimulated cell, becoming excited. In a third large region, the propagation condition is satisfied and all cells become excited via a regenerative calcium wave (Fig. 4). All other regions with $m > 1$ cells excited exist in between the upper boundary of the one-cell region and the boundary to intercellular waves (cf. Fig. 4 *b* for $m = 2$), but their size is negligible.

This behavior depends on the value of s; for considerably larger variation in s (100-fold and more), regions with $m > 1$ become noticeable. Also, for values of α just above 2 the critical permeabilities are much larger, and with this the regions for finite cell numbers becoming excited are enlarged. However, for realistic ranges for s and P, intercellular wave propagation in the model is practically an all-or-none phenomenon. Regenerative calcium waves are triggered if the propagation condition is satisfied; otherwise the signal remains restricted to the stimulated cell or its neighbors. This is also found in numerical simulations with smooth kinetics.

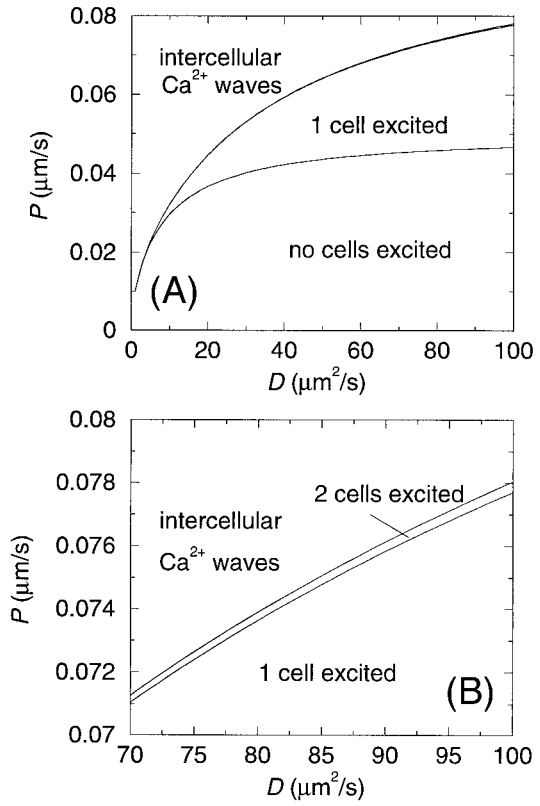

FIGURE 4 Range of spatially limited signals. (*a*) In the *D*-*P* plane for $\alpha = 100$ and the applied stimulus $s = 200$ (p.w.l. kinetics); (*b*) magnification of a region of (*a*). Conversion of p and δ to dimensional form as in Fig. 3.

Speed of propagation

A central quantity to be compared with experimental data is the speed of calcium wave propagation. For intercellular signals the speed is determined by the time taken by the wavefront to traverse the cell and the time spent to cross the gap junctions. Referring to these as intracellular delay, τ_{cyt}, and gap-junctional delay, τ_{gj}, respectively, the overall speed of propagation becomes

$$v = \frac{L}{\tau_{cyt} + \tau_{gj}}. \tag{30}$$

An estimate of the intracellular wave speed is obtained by calculating the speed at which a travelling front would propagate according to Eq. 7 if no cell boundaries were present (e.g., Murray, 1993). This yields

$$\tau_{cyt} = \text{const. } L/\sqrt{kD}, \tag{31}$$

where const. $= \sqrt{\alpha - 1}/(\alpha - 2)$ for the p.w.l. kinetics Eq. 9b.

A crude estimate for the time to reach the CICR threshold by gap-junctional calcium influx can be obtained for the p.w.l. kinetics from Eq. 27 by solving $u(0, t) = 1$ for t, at some value of $\hat{u}$. Expanding $u(0, t)$ for small times and taking $\hat{u} = \alpha$, one finds explicitly,

$$t = D\left(\frac{K_a k}{P\nu_m}\right)^2. \tag{32}$$

This expression gives an indication of the parameter dependence of τ_{gj}. In particular, Eq. 32 predicts an increase of τ_{gj} with calcium diffusivity, whereas Eq. 31 yields a decrease of τ_{cyt}. Correspondingly, we find numerically that the overall wave speed exhibits a maximum at intermediate values of D, for both types of kinetics in Eq. 9 (Fig. 5, *a* and *b*). The numerical results for the delays τ_{gj} and τ_{cyt} are shown in Fig. 5 *c*.

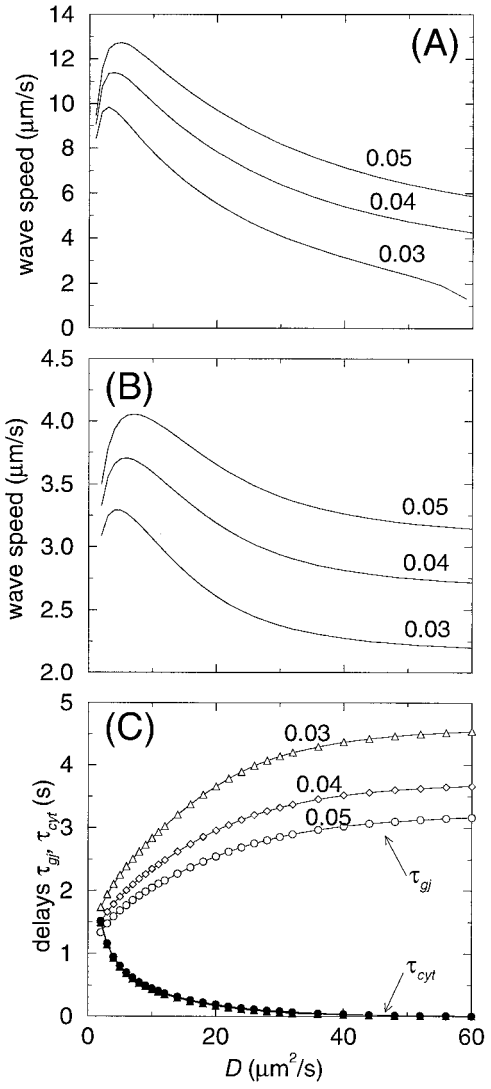

FIGURE 5 Speed of intercellular calcium waves and intracellular and gap-junctional delays. Wave speed (*a*) for piecewise linear kinetics ($\alpha = 225$); (*b*) for smooth kinetics ($\alpha = 15$), for the values of P indicated at the curves (in μm/s); (*c*) intercellular (τ_{gj}, *open symbols*) and intracellular (τ_{cyt}, *filled symbols*) delays for (*b*). Conversion of p and d to dimensional form as in Fig. 3.

In the rat liver, intercellular wave speeds and gap-junctional delays ranging between ~5–50 μm/s and 2–12 s, respectively, have been reported (Robb-Gaspers and Thomas, 1995); similar values are found in hepatocyte couplets (Combettes et al., 1994). In the blowfly salivary gland, intercellular speeds range between 10 and 20 μm/s (Zimmermann and Walz, 1999). Values for the wave speed in the model fall in the lower range of these experimental data (the cell length of 10 μm assumed in the calculations is actually rather low; somewhat larger speeds than in Fig. 5 would result for larger cells, as τ_{gj} is practically independent of cell length). The numerical values for the gap-junctional delay are also in agreement with the experimental data.

Experimental measurements of τ_{cyt} and τ_{gj} can be used in the model to estimate P and D. Computing the functions $\tau_{cyt}(\delta, p)$ and $\tau_{gj}(\delta, p)$ numerically, at fixed α, we found that the level curves τ_{cyt} = const. and τ_{gj} = const. in the (δ, p) plane have unique pairwise intersections. Hence a pair of values for the intracellular and intercellular delays corresponds to unique values for δ and p, conditional on a choice of α (Table 2). The resulting estimates of D agree with experimental data (Allbritton et al., 1992), and also P is within the accessible range, particularly for the larger intercellular delays of a few seconds.

Effects of parameter changes

The model allows the consequences of changes in cellular parameters to be evaluated. We focus on the effects of varying calcium buffer concentration and the cytoplasmic IP_3 level on the capacity for regenerative wave propagation and on the gap-junctional delay.

The results of changing the concentration of a calcium buffer depend on whether the buffer is diffusive ($D_j > 0$) or stationary ($D_j = 0$). Of the nondimensional parameter groupings Eq. 10, δ depends on diffusive buffers while α and p are independent of buffering. Therefore, the propagation condition Eq. 23 is independent of the concentration of stationary calcium buffers. By contrast, adding diffusive calcium buffer to a cell increases the critical calcium permeability and may thus shift the system from the regime of regenerative intercellular waves to failure of propagation (cf. Fig. 3). For the gap-junctional delay, we have approximately $\tau_{gj} \sim (D_0 + \Sigma D_j B_j/K_j)(1 + \Sigma B_j/K_j)$ from Eq. 32. Generally, addition of both diffusive and stationary calcium buffers causes an increase of τ_{gj}, which is greater for larger buffer diffusivity. If the calcium signals are of finite duration, it is conceivable that also changing the stationary buffer concentration may have effects other than altering the gap-junctional delay and wave speed.

The opening probability of the IP_3R increases with IP_3 concentration (Bezprozvanny and Ehrlich, 1995). Therefore the maximal rate of CICR, v_m, is an increasing function of the IP_3 concentration, and the effects of changes in IP_3 can be inferred qualitatively by changing v_m. The critical junctional calcium permeability for regenerative intercellular wave propagation decreases with increasing v_m (Fig. 6; Eq. 29). Alternatively, for a certain P, there will be a critical v_m and a corresponding IP_3 threshold. In the regime of wave propagation, the gap-junctional delay decreases with increasing IP_3 concentration (Fig. 7 *a*). For periodic calcium waves in the rat liver, Robb-Gaspers and Thomas (1995) indeed observed the gap-junctional delay to become smaller with increasing vasopression concentration. The numerically calculated dependence $\tau_{gj}(v_m)$ qualitatively follows the prediction of Eq. 32, as does the dependence of τ_{gj} on the junctional calcium permeability (Fig. 7 *b*).

TABLE 2 Effective calcium diffusion coefficient and gap-junctional permeabilities estimated from the model by assuming τ_{cyt} = 0.5 s and various τ_{gj}; α = 15, I = 0; conversion of p and δ to dimensional form as in Fig. 3

τ_{gj} (s)	D (μm^2/s)	P (μm/s)
1	12.4	0.3500
2	11.2	0.1225
5	10.4	0.0052

Asymmetric calcium signaling through gap junctions

Intercellular calcium signaling has been observed between different cell types, with potentially different values of cellular parameters (Hirata et al., 1998). Parameters can also vary within a cell population. Heterogeneity in calcium buffering, gap-junctional permeability, and CICR rate may affect the intercellular propagation of calcium signals. In particular, the model suggests mechanisms by which a calcium signal can spread from one type of cells to another, but not vice versa.

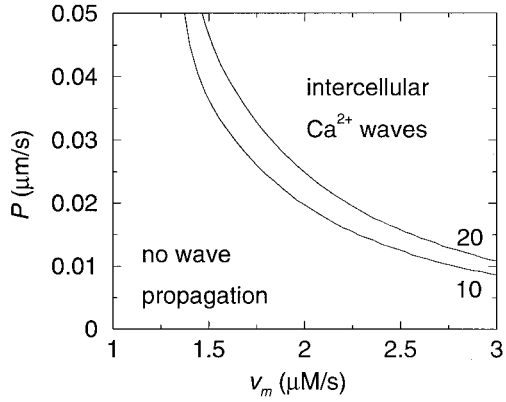

FIGURE 6 Critical gap-junctional calcium permeability P_c as a function of the maximal rate of CICR, v_m, for two different values of the calcium diffusivity as indicated at the curves (D in μm^2/s). Numerical result with kinetics Eq. 9a.

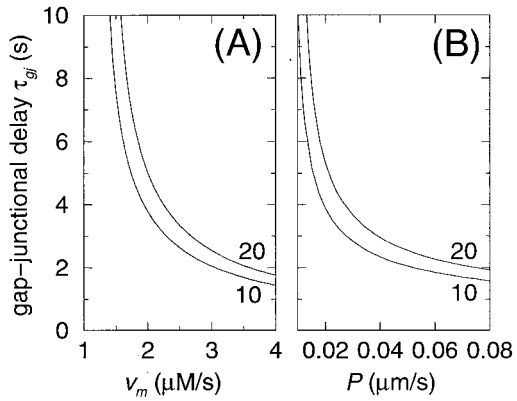

FIGURE 7 Dependence of the gap-junctional delay τ_{gj} on (*a*) maximal CICR rate v_m, and (*b*) on gap-junctional calcium permeability P. Numerical result with kinetics Eq. 9a; $P = 0.05$ μm/s in (*a*), $v_m = 3$ μM/s in (*b*); $D =$ 10 and 20 μm^2/s as indicated.

Consider two cell types, A and B, which differ with respect to the composition of cytoplasmic calcium buffers, and thus in their effective calcium diffusion coefficients. According to the propagation condition, signal propagation may be possible for a low calcium diffusivity (e.g., cell type A), but impossible for a larger diffusivity (cell type B). If a signal is evoked in cell type A, a calcium wave can spread among these cells but cannot cross the boundary to type B (transition from low to sufficiently high cytoplasmic calcium diffusivity is not possible). However, if a calcium signal is evoked in a cell B bordering a cell A, it will cross to this cell and spread among the A cells (transition from high to low calcium diffusivity is possible). If, in addition, the higher diffusivity among the cells B is compensated by a larger junctional permeability, than between A and B cells, then the situation depicted in Fig. 8 may arise. Here, calcium waves can propagate among A cells, B cells, from cells B to A, but not from cells A to B. Also, other constellations can result in asymmetric gap-junctional calcium signaling. For example, a smaller CICR rate constant v_m (smaller α) and a larger junctional permeability in B cells than in A cells can yield qualitatively the same result as in Fig. 8. These hypothetical mechanisms do not require asymmetry of gap-junctional permeabilities.

Finite distance between gap junctions and calcium stores

Up to now, we have focused on the case $l = d/L = 0$. The impact of a finite distance between gap junctions and the calcium release/uptake sites is illustrated in Fig. 9 for the p.w.l. form of $g(u)$; analogous results are obtained numerically with smooth $g(u)$. The junctional permeability required for intercellular waves decreases with increasing distance. In the limiting case $\delta \to \infty$, one obtains for the critical permeability from Eq. 12 $p_{c,\infty}(l) = (1 - 2l)p_{c,\infty}(0)$, where $p_{c,\infty}(0)$ is given by Eq. 24. For this behavior it may be critical that in the model the cytoplasmic calcium concentration reaches an elevated stationary state in the wake of the wave. As a consequence, calcium can flow from an activated cell into a nonactivated cell for an arbitrarily long time span. However, the return of calcium to its resting level in cells places an upper limit on the amount of calcium that can diffuse from an activated to a nonactivated cell, so that the threshold concentration for CICR may not be reached anymore if the distance to the calcium stores is too large. Preliminary results of numerical computations with a simple model in which calcium returns to the resting level indicate that in this situation larger gaps between gap junctions and calcium stores are no longer favorable for intercellular propagation. However, it appears that gaps of up to 1 μm that may be realistic in cells have little effect on the critical permeability.

DISCUSSION

We have investigated a basic mathematical model of intercellular calcium signal propagation by CICR and gap-junctional calcium diffusion. The model exhibits regenerative intercellular calcium waves for parameter values suggested by experimental data. In particular, the critical gap-junctional permeability required for wave propagation falls in a range reported in experimental studies.

Calcium buffering and removal preclude its action as a purely diffusive gap-junctional messenger over many cells. An estimate of the spatial range of a messenger within a cell is $r_m = \sqrt{D_m/k_m}$, where D_m and k_m are the diffusivity and first-order removal rate constant of the messenger, respectively (cf. Eq. 28). This yields $r_{Ca} \approx 3$–6 μm (Table 1). It is instructive to compare this with an estimate for IP_3, which is thought to mediate intercellular calcium waves in a number of systems by diffusion (Sanderson, 1995): $r_{IP_3} \approx 55$ μm ($D_{IP_3} = 300$ μm^2/s, Allbritton et al., 1992; $k_{IP_3} = 0.1$/s, Wang et al., 1995). Moreover, the junctional permeability for IP_3 can be expected to be in the range of P_0 (Table 1), whereas the effective calcium permeability is strongly reduced by calcium buffering (Eq. 6). Consequently, the spread of an intercellular calcium wave by gap-junctional calcium diffusion in the model requires the regeneration of the calcium signal in every cell. In experimental systems, this appears to be achieved by the global sensitization of IP_3R's toward CICR through IP_3 (Robb-Gaspers and Thomas, 1995; Zimmermann and Walz, 1999). Regeneration of the signal may also be carried by RyR's (Toyofuku et al., 1998). The triggering of CICR by gap-junctional calcium influx takes place in the vicinity of the gap junctions. This implies that intercellular propagation can be enhanced by mechanisms that lower the cytoplasmic diffusion rate of calcium (although these would, at the same time, slow the intracellular spread).

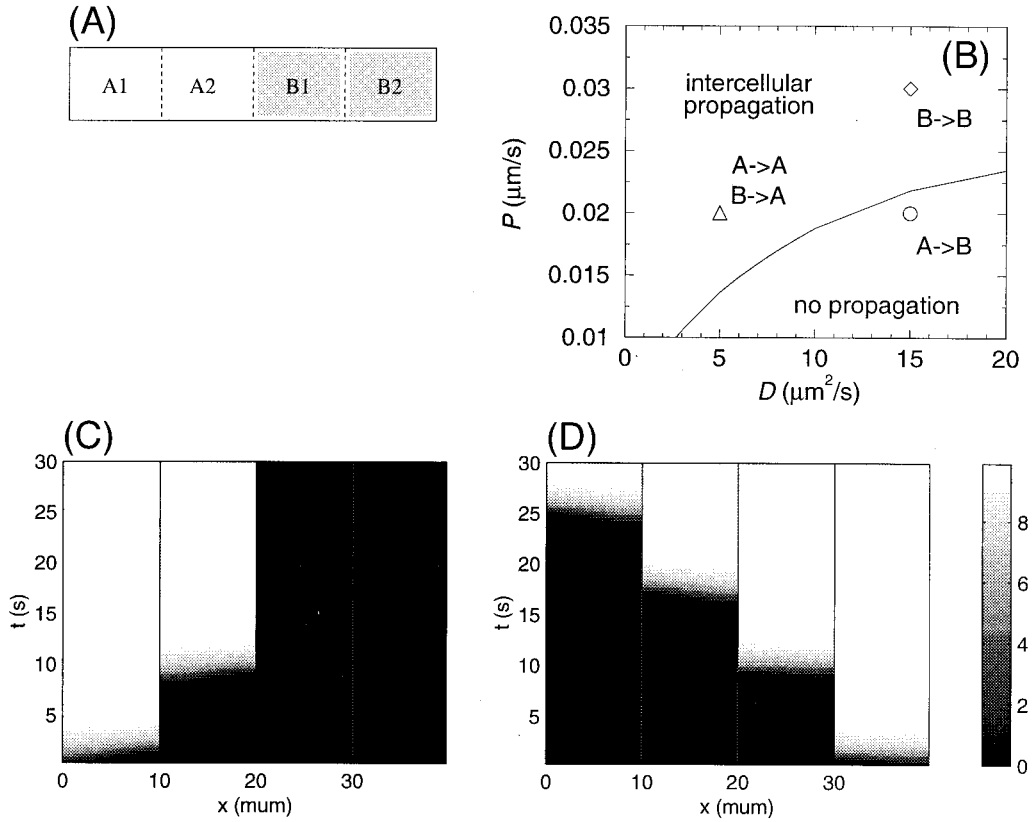

FIGURE 8 Asymmetric gap-junctional calcium signaling. (*a*) Array of four cells of two types with different junctional permeabilities (A: 0.02 μm/s, B: 0.03 μm/s) and effective cytoplasmic diffusion coefficients for calcium (A: 5 μm^2/s, B: 15 μm^2/s); junctional permeability between cells A2 and B1 0.02 μm/s; $\alpha = 10$ in A and B. (*b*) Critical curve for wave propagation taken from Fig. 3; propagation is possible between cells of the same type (◇, △) and from B to A (△), but not from A to B (○). Accordingly, a calcium signal elicited in cell A1 propagates to A2 but not to B1 (*c*), whereas a signal elicited in cell B2 spreads to cells B1, A2, and A1 (*d*). Calcium concentration scale in dimensionless units.

For the values of P_c obtained in the model, one may estimate the increase in calcium concentration by gap-junctional calcium influx from Eq. 28. $P = 0.1$ μm/s, $D = 10$ μm^2/s, $k = 1$/s, and a calcium concentration of 1 μM in the excited cell give a calcium elevation by 30 nM near the gap junctions in the yet unexcited cell. Larger elevations would result from a lower rate of calcium removal in the perijunctional space (e.g., 90 nM for $k = 0.1$/s). It is conceivable that the geometrical arrangement of calcium release and uptake sites near the gap junctions may be of importance for wave propagation, in addition to the factors investigated in this paper.

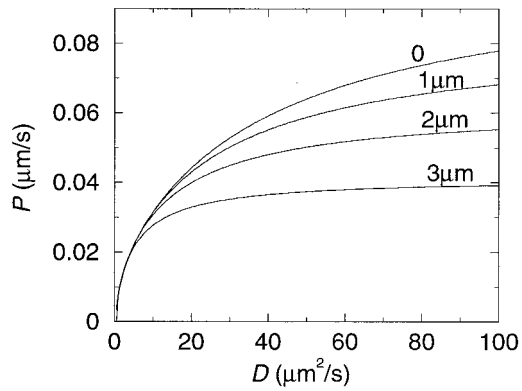

FIGURE 9 Critical permeability for the p.w.l. kinetics with a finite gap between gap junctions and calcium stores, $\alpha = 100$; conversion of p and δ to dimensional form as in Fig. 3; curves are labeled with the gap size d, cf. Eq. 4.

Because of the regenerative nature of the calcium waves, their spatial range of propagation is potentially arbitrarily large, only limited by system boundaries. The overall speed of propagation is constant. Very long-ranging calcium waves of constant speed were indeed reported for systems in which PLC-activating agonist has been applied globally, and junctional calcium diffusion has been hypothesized as the coupling mechanism (Cornell-Bell et al., 1990; Robb-Gaspers and Thomas, 1995; Zimmermann and Walz, 1999). By contrast, in systems in which IP_3 is thought to act as a purely diffusive intercellular messenger, calcium waves are usually of finite spatial extent, with the propagation speed declining in a radially outward direction (Sanderson, 1995). However, intercellular calcium waves propagated by CICR

and calcium diffusion could also be of a restricted spatial range because of factors not included in the present analysis. It is conceivable, for example, that the sensitization of the IP_3R toward CICR is of limited duration, as agonist receptors may desensitize upon global, long-lasting stimulation.

APPENDIX 1

Fast calcium buffering approximation

Calcium is bound to many proteins and other molecules in the cytoplasm. Binding to many of these can be considered fast when compared to calcium release and diffusion. Following Wagner and Keizer (1994), we apply a rapid-equilibrium approximation to calcium buffering in a somewhat variant form to include flux boundary conditions required for the gap-junctional fluxes.

Consider M different calcium binding sites with binding and dissociation rate constants k_j^+ and k_j^-, respectively. Each calcium-binding species is assumed to be homogeneously distributed throughout the cytoplasm, with a total concentration B_j; the concentrations of free and occupied binding sites are denoted by b_j and c_j, respectively. The calcium-binding molecules can diffuse. For simplicity, their diffusion coefficients D_j are taken not to depend on the number of bound calcium molecules; then homogeneity of the total concentrations B_j also implies the local conservation relation $b_j(x, t) + c_j(x, t) = B_j$. The dynamics of this system are described by

$$\frac{\partial u}{\partial t} = f_0(u) + \sum_{j=1}^{M}[k_j^- c_j - k_j^+(B_j - c_j)u] + D_0\frac{\partial^2 u}{\partial x^2} \tag{33}$$

$$\frac{\partial c_j}{\partial t} = -k_j^- c_j + k_j^+(B_j - c_j)u + D_j\frac{\partial^2 c_j}{\partial x^2}, \tag{34}$$

where $j = 1, \ldots, M$. D_0 and f_0 denote the diffusion coefficient of free calcium and the rate of ER release and uptake, respectively. In keeping with the model studied in this paper, we focus on a one-dimensional spatial domain $(0, L)$; the approach developed below can be generalized to two and three dimensions. There can be calcium fluxes across the boundaries $x = 0$ and $x = L$ through gap junctions, $j_{0,L}$, whereas the larger buffer molecules are confined to the cell. This results in the boundary conditions to Eqs. 33 and 34,

$$-D_0\frac{\partial u}{\partial x}\bigg|_{x=0,L} = j_{0,L}, \quad -D_j\frac{\partial c_j}{\partial x}\bigg|_{x=0,L} = 0. \tag{35}$$

The concentration of total (free and bound) calcium, $w = u + \Sigma_j c_j$, is governed by

$$\frac{\partial w}{\partial t} = f_0\left(w - \sum_{j=1}^{M} c_j\right) + D_0\frac{\partial^2 w}{\partial x^2} + \sum_{j=1}^{M}(D_j - D_0)\frac{\partial^2 c_j}{\partial x^2}, \tag{36}$$

with the boundary conditions

$$-D_0\frac{\partial w}{\partial x}\bigg|_{x=0,L} - \sum_{j=1}^{M}(D_j - D_0)\frac{\partial c_j}{\partial x}\bigg|_{x=0,L} = j_{0,L}. \tag{37}$$

We now make the assumption that calcium binding, determined by k_j^- and $k_j^+ B_j$, is fast compared to the release and uptake rate f_0, calcium diffusion, and buffer diffusion. Then calcium binding in Eq. 34 can be assumed to be in a quasi-equilibrium given by

$$c_j(u) = \frac{B_j u}{K_j + u}, \tag{38}$$

where $K_j = k_j^-/k_j^+$ is the dissociation constant of the jth binding site. Equation 36, unlike Eq. 33, does not involve the fast binding rates, so that w is the appropriate slow variable to describe the calcium dynamics. Inserting $u = w - \Sigma_j c_j$ in Eq. 38, one can solve (numerically) for the c_j as functions of w, $c_j = \phi_j(w)$. This yields Eq. 36 in the form

$$\frac{\partial w}{\partial t} = f_0\left(w - \sum_{j=1}^{M}\phi(w)\right) + \frac{\partial}{\partial x}\left[\left(D_0 + \sum_{j=1}^{M}(D_j - D_0)\phi_j'(w)\right)\frac{\partial w}{\partial x}\right], \tag{39}$$

with

$$-\left(D_0 + \sum_{j=1}^{M}(D_j - D_0)\phi_j'(w)\right)\frac{\partial w}{\partial x}\bigg|_{x=0,L} = j_{0,L}. \tag{40}$$

The diffusion coefficient for total calcium is $D_0 + \Sigma_j(D_j - D_0)\phi_j'(w)$. Many calcium-binding molecules have low calcium affinity in the micromolar range and above (Neher and Augustine, 1992), so that we furthermore assume $u \ll K_j$. Then Eq. 38 can be approximated by $c_j(u) = uB_j/K_j$, so that $w = (1 + \Sigma_j B_j/K_j)u$ and $\phi_j(w) = wB_j/K_j/(1 + \Sigma_l B_l/K_l)$. With these relations, Eq. 39 can be rewritten in terms of u, to obtain Eq. 1 (with $u_i = u$),

$$\frac{\partial u}{\partial t} = f(u) + D\frac{\partial^2 u}{\partial x^2},$$

where we have introduced the effective calcium release/uptake rate $f(u)$

$$f(u) = f_0(u)\Big/\left(1 + \sum_{j=1}^{M} B_j/K_j\right), \tag{41}$$

and the effective diffusion coefficient D

$$D = \left(D_0 + \sum_{j=1}^{M} D_j B_j/K_j\right)\Big/\left(1 + \sum_{j=1}^{M} B_j/K_j\right). \tag{42}$$

The boundary conditions 40 become

$$-D\frac{\partial u}{\partial x}\bigg|_{0,L} = \frac{j_{0,L}}{1 + \sum_{j=1}^{M} B_j/K_j}, \tag{43}$$

so that we also define the effective gap-junctional permeability for calcium

$$P = P_0 \Big/ \left(1 + \sum_{j=1}^{M} B_j/K_j\right), \quad (44)$$

where P_0 is the permeability in the absence of buffering. With this definition, Eq. 43 gives rise to the boundary conditions 5, completing the derivation of the fast calcium-buffering approximation.

APPENDIX 2

Numerical method

The solution to Eqs. 7–9 is approximated using an explicit Euler method on an equally spaced spatial grid of K grid points for each cell. Let $u_{i,j}^k$ be the value of the numerical solution for $u_i(\xi, \tau)$ at $\xi = (j - 1/2)/K$, $j = 1, \ldots, K$, and $\tau = k\Delta t$, where Δt is the time increment. For an inner point of a cell, $2 \le j \le K - 1$, we have the usual

$$u_{i,j}^{k+1} = u_{i,j}^k + \Delta t(g(u_{i,j}^k) + K^2\delta(u_{i,j-1}^k - 2u_{i,j}^k + u_{i,j+1}^k)), \quad i = 0, 1, \ldots, n, \quad (45)$$

while for boundary points, a first-order approximation of the fluxes across the gap junctions using the two adjacent grid points yields (cf. Sneyd et al., 1995)

$$u_{i,1}^{k+1} = u_{i,1}^k + \Delta t(g(u_{i,1}^k) + K^2\delta(u_{i,2}^k - (1 + \tilde{p})u_{i,1} + \tilde{p}u_{i-1,K}^k)), \quad i > 0 \quad (46)$$

$$u_{i,K}^{k+1} = u_{i,K}^k + \Delta t(g(u_{i,K}^k) + K^2\delta(u_{i,K-1}^k - (1 + \tilde{p})u_{i,K} + \tilde{p}(u_{i+1,1}^k)), \quad i < n \quad (47)$$

where

$$\tilde{p} = \frac{p/K}{\delta + p/K} \quad (48)$$

The boundary conditions were $u_{0,1}^k = s$ and zero flux conditions at the right end of the array. The calculations of p_c in Fig. 3 and of the wave speed were carried out on an array of 10 cells, with $K = 80$ and $\Delta t = 0.4\delta/K^2$. As the transition from one excited cell to nondecaying waves turned out to be very sharp, this domain length proved sufficient. In each case $s = u_a$.

The authors thank Dr. C. Giaume and Dr. L. Venance for stimulating discussions.

REFERENCES

Allbritton, N. L., T. Meyer, and L. Stryer. 1992. Range of messenger action of calcium-ion and inositol 1,4,5-trisphosphate. *Science.* 258: 1812–1815.

Berridge, M. J. 1997. Elementary and global aspects of calcium signalling. *J. Physiol.* 499:291–306.

Bezprozvanny, I., and B. E. Ehrlich. 1995. The inositol 1,4,5-trisphosphate ($InsP_3$) receptor. *J. Membr. Biol.* 145:205–216.

Bruzzone, R., T. W. White, and D. L. Paul. 1996. Connections with connexins: the molecular basis of direct intercellular signaling. *Eur. J. Biochem.* 238:1–27.

Charles, A. C., C. C. G. Naus, D. G. Zhu, G. M. Kidder, E. R. Dirksen, and M. J. Sanderson. 1992. Intercellular calcium signaling via gap junctions in glioma cells. *J. Cell Biol.* 118:195–201.

Christ, G. J., A. P. Moreno, A. Melman, and D. C. Spray. 1992. Gap junction-mediated intercellular diffusion of Ca^{2+} in cultured human corporal smooth muscle cells. *Am. J. Physiol. Cell Physiol.* 263: C373–C383.

Combettes, L., D. Tran, T. Tordjmann, M. Laurent, B. Berthon, and M. Claret. 1994. Ca^{2+}-mobilizing hormones induce sequentially ordered Ca^{2+} signals in multicellular systems of rat hepatocytes. *Biochem. J.* 304:585–594.

Cornell-Bell, A. H., S. M. Finkbeiner, M. S. Cooper, and S. J. Smith. 1990. Glutamate induces calcium waves in cultured astrocytes: long-range glial signaling. *Science.* 247:470–473.

Crank, J. 1975. The Mathematics of Diffusion, 2nd Ed. Oxford University Press.

D'Andrea, P., and F. Vittur. 1997. Propagation of intercellular Ca^{2+} waves in mechanically stimulated articular chondrocytes. *FEBS Lett.* 400: 58–64.

Daub, B., and V. Y. Ganitkevitch. 2000. An estimate of rapid cytoplasmic calcium buffering in single smooth muscle cells. *Cell Calcium.* 27:3–13.

Domenighetti, A. A., J. L. Bény, F. Chabaud, and M. Frieden. 1998. An intercellular regenerative calcium wave in porcine coronary artery endothelial cells in primary culture. *J. Physiol.* 513:103–116.

Dufour, J., I. M. Arias, and T. J. Turner. 1997. Inositol 1,4,5-trisphosphate and calcium regulate the calcium release channel function of the hepatic inositol 1,4,5-trisphosphate receptor. *J. Biol. Chem.* 272:2675–2681.

Dupont, G., and A. Goldbeter. 1993. A one-pool model for Ca^{2+} oscillations involving Ca^{2+} and inositol 1,4,5-trisphosphate as co-agonists for Ca^{2+} release. *Cell Calcium.* 14:311–322.

Eckert, R., B. Adams, J. Kistler, and P. Donaldson. 1999. Quantitative determination of gap junctional permeability in the lens cortex. *J. Membr. Biol.* 169:91–102.

Fabiato, A. 1985. Time and calcium dependence of activation and inactivation of calcium-induced release of calcium from the sarcoplasmic reticulum of a skinned canine cardiac Purkinje cell. *J. Gen. Physiol.* 85:247–289.

Giaume, C., and K. D. McCarthy. 1996. Control of gap-junctional communication in astrocyte networks. *Trends Neurosci.* 19:319–325.

Giaume, C., and L. Venance. 1998. Intercellular calcium signalling and gap junctional communication in astrocytes. *Glia.* 24:50–64.

Hagar, R. E., A. D. Burgstahler, M. H. Nathanson, and B. E. Ehrlich. 1998. Type III InsP(3) receptor channel stays open in the presence of increased calcium. *Nature.* 396:81–84.

Hassinger, T. D., P. B. Guthrie, P. B. Atkinson, M. V. L. Bennett, and S. B. Kater. 1996. An extracellular signaling component in propagation of astrocytic calcium waves. *Proc. Natl. Acad. Sci. USA.* 93:13268–13273.

Hirata, K., M. H. Nathanson, and M. L. Sears. 1998. Novel paracrine signaling mechanism in the ocular ciliary epithelium. *Proc. Natl. Acad. Sci. USA.* 95:8381–8386.

Höfer, T. 1999. Model of intercellular calcium oscillations in hepatocytes: synchronization of heterogeneous cells. *Biophys. J.* 77:1244–1256.

Kaftan, E. J., B. Ehrlich, and J. Watras. 1997. Inositol 1,4,5-trisphosphate ($InsP_3$) and calcium interact to increase the dynamic range of $InsP_3$ receptor-dependent calcium signaling. *J. Gen. Physiol.* 110:529–538.

Keener, J. P. 1987. Propagation and its failure in coupled systems of excitable cells. *SIAM J. Appl. Math.* 47:556–572.

Lloréns, M., J. C. Nuño, Y. Rodriguez, E. Meléndez-Hevia, and F. Montero. 1999. Generalization of the theory of transition times in metabolic pathways: a geometrical approach. *Biophys. J.* 77:23–36.

Meissner, G. 1994. Ryanodine receptor Ca^{2+} release channels and their regulation by endogenous effectors. *Annu. Rev. Physiol.* 56:485–508.

Murray, J. D. 1993. Mathematical Biology. Springer-Verlag, Berlin.

Neher, E., and G. J. Augustine. 1992. Calcium gradients and buffers in bovine chromaffin cells. *J. Physiol.* 450:273–301.

Patel, S., L. D. Robb-Gaspers, K. A. Stellato, M. Shon, and A. P. Thomas. 1999. Coordination of calcium signalling by endothelial-derived nitric oxide in the intact liver. *Nat. Cell Biol.* 1:467–471.

Robb-Gaspers, L. D., and A. P. Thomas. 1995. Coordination of Ca^{2+} signaling by intercellular propagation of Ca^{2+} waves in the intact liver. *J. Biol. Chem.* 270:8102–8107.

Sáez, J. C., J. A. Connor, D. C. Spray, and M. V. L. Bennett. 1989. Hepatocyte gap junctions are permeable to the second messenger, inositol 1,4,5-trisphosphate, and to calcium ions. *Proc. Natl. Acad. Sci. USA.* 86:2708–2712.

Sanderson, M. J. 1995. Intercellular calcium waves mediated by inositol trisphosphate. *CIBA Found. Symp.* 188:175–189.

Schlosser, S. F., A. D. Burgstahler, and M. H. Nathanson. 1996. Isolated rat hepatocytes can signal to other hepatocytes and bile duct cells by release of nucleotides. *Proc. Natl. Acad. Sci. USA.* 93:9948–9953.

Sneyd, J., B. T. R. Wetton, A. C. Charles, and M. J. Sanderson. 1995. Intercellular calcium waves mediated by diffusion of inositol trisphosphate: a 2-dimensional model. *Am. J. Physiol. Cell Physiol.* 37:C1537–C1545.

Thomas, A. P., G. S. J. Bird, G. Hajnoczky, L. D. Robb-Gaspers, and J. W. Putney. 1996. Spatial and temporal aspects of cellular of calcium signalling in hepatocytes. *FASEB J.* 10:1505–1517.

Tjordmann, T., B. Berthon, M. Claret, and L. Combettes. 1997. Coordinated intercellular calcium waves induced by noradrenaline in rat hepatocytes: dual control by gap junction permeability and agonist. *EMBO J.* 16:5398–5407.

Tordjmann, T., B. Berthon, E. Jacquemin, C. Clair, N. Stelly, G. Guillon, M. Claret, and L. Combettes. 1998. Receptor-oriented intercellular calcium waves evoked by vasopressin in rat hepatocytes. *EMBO J.* 17: 4695–4703.

Toyofuku, T., M. Yabuki, K. Otsu, T. Kuzuya, M. Hori, and M. Tada. 1998. Intercellular calcium signaling via gap junction in connexin-43 transfected cells. *J. Biol. Chem.* 273:1519–1528.

Verselis, V., R. L. White, D. C. Spray, and M. V. L. Bennett. 1986. Gap junctional conductance and permeability are linearly related. *Science.* 234:461.

Wagner, J., and J. Keizer. 1994. Effects of rapid buffers on Ca^{2+} diffusion and Ca^{2+} oscillations. *Biophys. J.* 67:447–456.

Wang, S. S. H., A. A. Alousi, and S. H. Thompson. 1995. The lifetime of inositol 1,4,5-trisphosphate in single cells. *J. Gen. Physiol.* 105: 149–171.

Wang, Z., M. Tymianski, O. T. Jones, and M. Nedergaard. 1997. Impact of cytoplasmic calcium, buffering on the spatial and temporal characteristics of intercellular calcium signals in astrocytes. *J. Neurosci.* 17: 7359–7371.

Wilkins, M., and J. Sneyd. 1998. Intercellular spiral waves of calcium. *J. Theor. Biol.* 191:299–308.

Yule, D. I., E. Stuenkel, and J. A. Williams. 1996. Intercellular calcium waves in rat pancreatic acini: mechanisms of transmission. *Am. J. Physiol. Cell Physiol.* 40:C1285–C1294.

Zimmermann, B., and B. Walz. 1999. The mechanism mediating regenerative intercellular Ca^{2+} waves in the blowfly salivary gland. *EMBO J.* 18:3222–3231.